Journal of Coordination Chemistry
Publication details, including instructions for authors and subscription information:
http://www.tandfonline.com/loi/gcoo20

DNA-binding and photocleavage of fluorescein-porphyrinatozinc complexes

Jiazheng Lu [a], Haiwei Guo [a], Yongli Zhang [b], Jing Jiang [a c], Yunjin Liu [a], Linquan Zang [a] & Jinwang Huang [c]

[a] School of Pharmacy, Guangdong Pharmaceutical University, Guangzhou 510006, People's Republic of China

[b] School of Basic Courses, Guangdong Pharmaceutical University, Guangzhou 510006, People's Republic of China

[c] State Key Laboratory of Optoelectronic Material and Technologies & School of Chemistry and Chemical Engineering, Sun Yat-Sen University, Guangzhou 510275, People's Republic of China

Published online: 23 Apr 2012.

To cite this article: Jiazheng Lu, Haiwei Guo, Yongli Zhang, Jing Jiang, Yunjin Liu, Linquan Zang & Jinwang Huang (2012) DNA-binding and photocleavage of fluorescein-porphyrinatozinc complexes, Journal of Coordination Chemistry, 65:10, 1765-1780, DOI: 10.1080/00958972.2012.681381

To link to this article: http://dx.doi.org/10.1080/00958972.2012.681381

Journal of Coordination Chemistry
Vol. 65, No. 10, 20 May 2012, 1765–1780

DNA-binding and photocleavage of fluorescein-porphyrinatozinc complexes

JIAZHENG LU*†, HAIWEI GUO†, YONGLI ZHANG‡, JING JIANG†§, YUNJIN LIU†, LINQUAN ZANG† and JINWANG HUANG§

†School of Pharmacy, Guangdong Pharmaceutical University, Guangzhou 510006, People's Republic of China
‡School of Basic Courses, Guangdong Pharmaceutical University, Guangzhou 510006, People's Republic of China
§State Key Laboratory of Optoelectronic Material and Technologies & School of Chemistry and Chemical Engineering, Sun Yat-Sen University, Guangzhou 510275, People's Republic of China

(*Received 6 August 2011; in final form 5 March 2012*)

Three fluorescein-porphyrinatozinc(II) complexes, Zn(Fl-HPTTP) (**1**) (Fl-HPTTP = 5-(4-fluoresceinhexyloxy)phenyl-10,15,20-tritolylporphyrin), Zn(Fl-HPTPP) (**2**) (Fl-HPTPP = 5-(4-fluoresceinhexyloxy)phenyl-10,15,20-triphenylporphyrin), and Zn(Fl-HPTCPP) (**3**) (Fl-HPTCPP = 5-(4-fluoresceinhexyloxy)phenyl-10,15,20-tri(4-chloro)phenylporphyrin), have been synthesized and characterized by elemental analysis, IR, UV-Vis, ES-MS, and ^{1}H NMR. The DNA-binding behaviors of these complexes with calf-thymus DNA (*ct*-DNA) were investigated by UV-Vis absorption titration, fluorescence spectra, viscosity measurements, thermal denaturation, and circular dichroism. The results suggest that **1**, **2**, and **3** interact with *ct*-DNA by intercalation and the DNA-binding affinities of these fluorescein-porphyrinatozinc(II) complexes may be closely associated with electronic effects of the substituent group introduced on the porphyrin ring of the ligands. The DNA-binding affinity (K_b values) follows the order **1** > **2** > **3**. In addition, their photocleavage reactions with pBR322 supercoiled plasmid DNA were investigated by gel electrophoresis experiments. All complexes exhibit significant DNA cleavage activity. The cleavage ability of the fluorescein-porphyrinatozinc(II) complexes follows the order **1** > **2** > **3**, in parallel to the magnitude of their intrinsic binding constants.

Keywords: Fluorescein; Porphyrinatozinc; Complex; DNA-binding; Photocleavage

1. Introduction

Porphyrins perform a wide variety of functions in natural and synthetic systems. Owing to their special photophysical and electrochemical properties, remarkable stability, and well-known structure, porphyrins and metallo-porphyrins have been frequently used as building blocks for the construction of artificial systems with special built-in properties or functions [1–7]. Porphyrin is selectively taken up by tumor cells [8–10]. Because of

*Corresponding author. Email: lujia6812@163.com

ISSN 0095-8972 print/ISSN 1029-0389 online © 2012 Taylor & Francis
http://dx.doi.org/10.1080/00958972.2012.681381

this property, porphyrin has been used as a tumor targeting agent in photodynamic therapy (PDT) [11–13]. PDT, in which light activates a photosensitizing drug and elicits the $^1O_2$ mediated cytotoxic action, has emerged as a promising modality against cancer and allied diseases [12, 14–17].

Porphyrins and their derivatives are also among the most studied DNA-binding agents [6, 7, 18–20], extensively studied since Fiel and colleagues discovered that these compounds can form various complexes with DNA [8, 21–23]. Currently, hematoporphyrin derivative (or its commercial variant Photofrin II) is the most widely used photosensitizer in PDT. However, application of this drug is known to cause undesirable, post-treatment phototoxic response, probably due to non-specific subcellular level activity during its photodynamic action [24, 25]. A possible way to circumvent this problem involves the use of targeted drug delivery. There are some reports about the synthesis of photoactive porphyrins which bind selectively to DNA owing to their linkage to either an intercalator [5–7] (e.g., acridone, phenothiazine), a minor groove binder [8, 9] (e.g., ellipticine) or a cross-linking agent [7–10, 26] (e.g., chorambucil). Binding can be either intercalative or external, in the minor groove (in some special cases with self-stacking), depending on the charge distribution of the porphyrin and the type of the metal in the porphyrin and on peripheral substituents [9, 27]. Utilization of a photoactive, intercalate moiety in conjunction with the porphyrin chromophore might accentuate the photochemical activity of the so-derived hybrid molecules, leading to efficient DNA-binding and DNA cleavage. Among the various non-porphyrinic chromophores that can be linked to porphyrin in such new hybrids, fluorescein seemed to be an ideal candidate because it is an ubiquitous electron acceptor [28–31]. However, little attention has been paid to study fluorescein-conjugated metallo-porphyrins interactions with DNA.

Herein, we report synthesis and characterization of three fluorescein-porphyrinato-zinc complexes Zn(Fl-HPTTP) (**1**) (Fl-HPTTP = 5-(4-fluoresceinhexyloxy)phenyl-10, 15,20-tritoylporphyrin), Zn(Fl-HPTPP) (**2**) (Fl-HPTPP = 5-(4-fluoresceinhexyloxy) phenyl-10,15,20-triphenylporphyrin), and Zn(Fl-HPTCPP) (**3**) (Fl-HPTCPP = 5-(4-fluoresceinhexyloxy)phenyl-10,15,20-tri(4-chloro)phenylporphyrin). The interactions of these three complexes with calf-thymus DNA (*ct*-DNA) were investigated using UV-Vis absorption titration, fluorescence spectra, viscosity measurements, thermal denaturation, and circular dichroism (CD). Photocleavage reactions with pBR322 supercoiled plasmid DNA were investigated by gel electrophoresis experiments. These results help understand interactions between DNA and metallo-porphyrins, which may facilitate design of new anticancer drugs.

2. Experimental

2.1. *Materials and methods*

$CHCl_3$ and other chemicals used in the synthesis and physical measurements were purified prior to use by published methods [28–30].

Disodium salt of *ct*-DNA (Sigma) was used as received. A solution of *ct*-DNA in buffer I gave a ratio of UV absorbance at 260 and 280 nm of 1.8–1.9 : 1, indicating that the DNA was sufficiently free of protein [31, 32]. The DNA concentration per

nucleotide was determined by absorption spectroscopy using the molar absorption coefficient (6600 $(\text{mol L}^{-1})^{-1}\,\text{cm}^{-1}$) at 260 nm [24, 33–35]. Stock solutions were stored at 4°C and used after no more than 4 days. pBR 322 DNA was also purchased from Sigma and used without purification. Other materials were of analytical reagent grade and used without purification unless otherwise noted.

Buffer I, 5 mmol L^{-1} Tris-HCl/50 mmol L^{-1} NaCl in water (pH = 7.0), was used for absorption titration, fluorescence spectra, viscosity measurements, thermal denaturation, and CD. Buffer II, 50 mmol L^{-1} Tris-HCl/18 mmol L^{-1} NaCl in water (pH = 7.2), was used for DNA-binding studies and gel electrophoresis experiments. Buffer III, Tris-boric acid-EDTA in water (pH = 8.3), was used for gel electrophoresis experiments. A phosphoric acid buffer containing 1.5 mmol L^{-1} Na_2HPO_4, 0.5 mmol L^{-1} NaH_2PO_4, and 0.25 mmol L^{-1} Na_2H_2EDTA ($H_4EDTA = N,N'$-ethane-1,2-diylbis[*N*-(carboxymethyl)glycine]) (pH = 7.0) was used for thermal denaturation.

2.2. *Physical measurements*

Microanalyses (C, H, and N) were carried out with a Perkin-Elmer 240Q elemental analyzer. Electrospray mass spectra (ES-MS) were recorded on an LCQ system (Finnigan MAT, USA) using methanol as the mobile phase. ^{1}H NMR spectra were recorded on a Varian-500 spectrometer. All chemical shifts are given relative to tetramethylsilane. Infrared (IR) spectra were recorded on a Bomen FTIR model MB102 instrument using KBr pellets. UV-Vis spectra were recorded on a Schimadzu UV-3101 PC spectrophotometer at room temperature. Emission spectra were recorded on a Perkin-Elmer Lambda 55 spectrofluorophotometer. CD spectra were recorded on a JASCO-J810 spectrometer.

2.3. *DNA-binding studies*

Absorption titration of fluorescein-porphyrinatozinc(II) complexes in tris-HCl buffer was performed by using a fixed concentration of the fluorescein-porphyrinatozinc(II) complexes (20 μmol L^{-1}) to which DNA stock solution was added. Fluorescein-porphyrinatozinc(II)-DNA solution was allowed to incubate for 3 min before absorption spectra were recorded. To further elucidate the binding strength of the complex, the intrinsic binding constant K_b with *ct*-DNA was obtained by monitoring the change in absorbance of the ligand transfer band with increasing amounts of DNA. The intrinsic binding constant K_b of the complex to DNA was calculated by using the following equation [20, 32–36]:

$$\frac{[\text{DNA}]}{\varepsilon_a - \varepsilon_f} = \frac{[\text{DNA}]}{\varepsilon_a - \varepsilon_f} + \frac{1}{K_b(\varepsilon_b - \varepsilon_f)},$$

where [DNA] is the concentration of DNA in base pairs, ε_a, ε_f, and ε_b refer to the corresponding apparent absorption coefficient $A_{obsd}/[\text{Zn(Fl-Por)}]$, the extinction coefficient for the free fluorescein-porphyrinatozinc(II) complex and the extinction coefficient for the fluorescein-porphyrinatozinc(II) complex in the fully bound form, respectively. In plots of $[\text{DNA}]/(\varepsilon_a - \varepsilon_f)$ *versus* [DNA], K_b is obtained by the ratio of the slope to the intercept.

Viscosity measurements were carried out using an Ubbelohde viscometer maintained at $28 \pm 0.1^{\circ}C$ in a thermostatic bath. The concentration of DNA was $0.5\,mmol\,L^{-1}$ in NP. Flow time was measured with a digital stopwatch and each sample was measured five times to obtain the average flow time. Data were presented as $(\eta/\eta_0)^{1/3}$ *versus* binding ratio [21, 33], where η is the viscosity of DNA in the presence of complexes while η_0 is the viscosity of DNA alone. Viscosity values were calculated from the observed flow time of DNA-containing solution ($t > 100\,s$) corrected for the flow time of buffer alone (t_0), $\eta = t - t_0/t_0$ [34, 36].

Thermal denaturation studies were carried out with a Schimadzu UV-3101 PC spectrophotometer equipped with a Peltier temperature-controlling programmer ($\pm 0.1^{\circ}C$). The melting curves were obtained by measuring the absorbance at 260 nm for solutions of *ct*-DNA ($100\,\mu mol\,L^{-1}$) in the absence and presence of different concentrations of the fluorescein-porphyrinatozinc(II) complexes as a function of temperature. The temperature was scanned from $40^{\circ}C$ to $92^{\circ}C$ at a speed of $1^{\circ}C\,min^{-1}$. The melting temperature (T_m) was taken as the midpoint of the hyperchromic transition.

The CD spectra of **1**, **2**, and **3** in the absence and presence of *ct*-DNA were performed on a JASCO-J810 spectrometer using a fixed concentration of the fluorescein-porphyrinatozinc(II) complex [Zn(Fl-Por)] = $10\,\mu mol\,L^{-1}$, and [DNA] = $130\,\mu mol\,L^{-1}$, respectively. Spectra were recorded at $25^{\circ}C$ after samples had been incubated with *ct*-DNA for 24 h at $37^{\circ}C$.

2.4. *Photoinduced cleavage of pBR 322 DNA by fluorescein-porphyrinatozinc(II) complexes*

For the gel electrophoresis experiments, pBR322 supercoiled plasmid DNA $0.5\,\mu L$ ($100\,\mu mol\,L^{-1}$ DNA-nucleotide) in tris-HCl buffer (pH = 7.2) was treated with $1.0\,\mu mol\,L^{-1}$ fluorescein-porphyrinatozinc(II) complex which was dissolved in dimethyl sulfoxide (DMSO). The mixture was incubated for an hour and the solutions were then irradiated with a high pressure mercury lamp (irradiation at 365 nm, 40 W, 25 cm above the solution surface) at room temperature for 60 min. The samples were analyzed for 30 min at 40 V in Buffer III containing 1% agarose gel. The gel was stained using $1\,mg\,mL^{-1}$ ethidium bromide (EB) and photographed under UV light.

2.5. *Synthesis and characterization*

2.5.1. Synthesis of 5-(4-fluoresceinhexyloxy)phenyl-10,15,20-tritolylporphyrin (Fl-HPTTP). Fl-HPTTP was synthesized according to a similar procedure to the literature method [29–31]. The synthetic route is shown in scheme 1. A mixture of 5-(4-bromohexyloxy) phenyl10,15,20-tritolylporphyrin (BrHPTTP) compound **1** (0.113 g, 0.129 mmol), fluorescein (0.2 g, 0.65 mmol), DMF ($25\,cm^3$), KF (0.5 g), and KI (0.05 g) was stirred for 48 h at $35^{\circ}C$ under nitrogen. The mixture was diluted with $50\,cm^3$ $CHCl_3$. The organic layer was washed with water ($5 \times 50\,cm^3$), dried with anhydrous Na_2SO_4, and concentrated by rotary evaporation. The residue was then chromatographed on a silica gel column using $CHCl_3$ as eluent to give four bands. The third band was collected and stripped on a rotary evaporator. The crude products were further purified by TLC

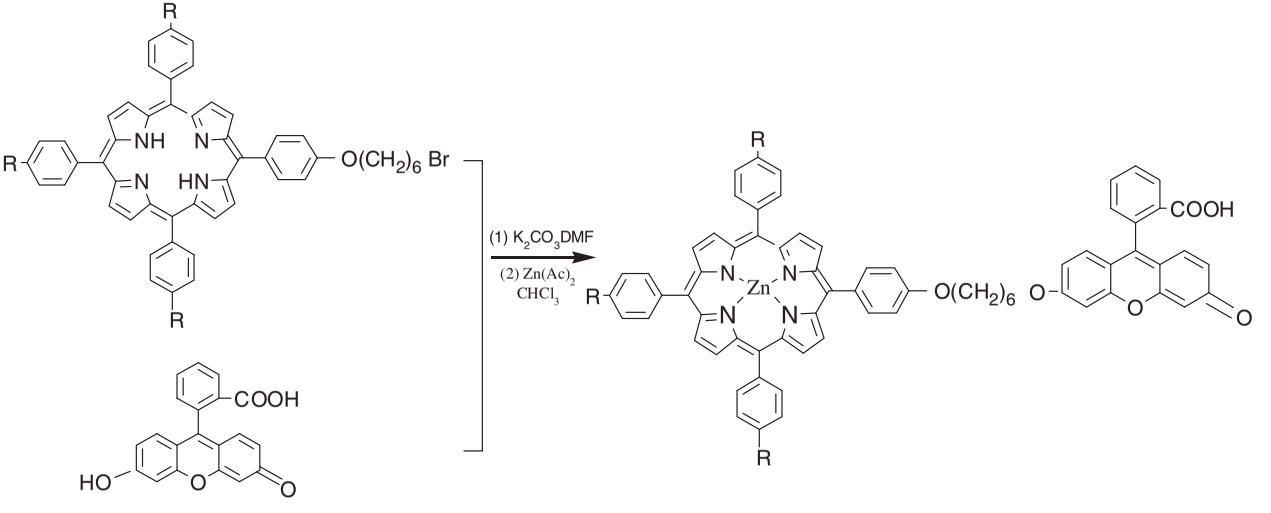

1 R= CH_3, 2 R = H, 3 R = Cl

Scheme 1. Synthesis of fluorescein-porphyrinatozinc(II).

to yield a purple solid. TLC was performed on Merck TLC plates silica gel 60 F_{254} utilizing UV light (254 nm). The yield of Fl-HPTTP was 54.3%. Elemental Anal. Calcd for $C_{73}H_{58}N_4O_6$ (%): C, 80.7; H, 5.3; N, 5.3. Found (%): C, 80.5; H, 5.1; N, 5.2. ^{1}H NMR (500 Hz, DMSO, ppm): δ 11.22 (1H, s, COOH), 8.72–8.95 (8H, m, 6-H), 8.2–8.65 (6H, d, 4-H, $J = 8.2$ Hz), 7.84–7.98 (2H, d, 2-H, $J = 8.0$ Hz), 7.7–7.82 (17H, m, 1,3,5-H), 7.21–7.50 (4H, d, 10,11,12-H, $J = 8.2$ Hz), 6.23–6.90 (6H, m, 13-H), 3.92–4.51 (2H, t, 7-H, $J = 8.4$ Hz), 3.48 (8H, t, 8-H, $J = 7.9$ Hz), 1.93 (2H, t, 9-H), −2.91 (s, 2H, pyrrole ring). IR (KBr pellets, ν_{max}/cm^{-1}): 3315 (porphyrin N–H), 2950–2858 (C–H), 1723 (carboxyl, C=O), 1640.2 (C=O), 1593.3 (C=C), and 1258–1218 (Ar–O–C) cm^{-1}. UV-Vis. (CH_2Cl_2, λ_{max} (nm), ε ($(mol\,L^{-1})^{-1}\,cm^{-1}$)): 420 ($1.21 \times 10^5$), 550 ($5.95 \times 10^3$), 598 ($2.22 \times 10^3$), and 645 ($1.25 \times 10^3$). ES-MS: m/z 1086.30 (M^+).

2.5.2. 5-(4-Fluoresceinhexyloxy)phenyl-10,15,20-triphenylporphyrin (Fl-HPTPP). Fl-HPTPP was prepared in a similar way to that of Fl-HPTTP except for 5-(4-bromohexyloxy)phenyl-10,15,20-triphenylporphyrin (BrHPTPP) instead of BrHPTTP. The yield of Fl-HPTPP was 52.3%. Elemental Anal. Calcd for $C_{70}H_{52}N_4O_6$ (%): C, 80.2; H, 5.0; N, 5.4. Found (%): C, 80.1; H, 5.0; N, 5.2. ^{1}H NMR (500 Hz, DMSO, ppm): δ 11.20 (1H, s, COOH), 8.76–8.95 (8H, m, 6-H), 8.2–8.5 (6H, d, 4-H, $J = 8.2$ Hz), 7.86–7.97 (2H, d, 2-H, $J = 7.8$ Hz), 7.80–7.85 (11H, m, 1,3,5-H), 7.23–7.54 (4H, d, 10,11,12-H, $J = 7.9$ Hz), 6.21–6.90 (6H, m, 13-H), 3.90–4.50 (2H, t, 7-H, $J = 6.9$ Hz), 3.45 (8H, t, 8-H, $J = 8.0$ Hz), 1.91 (2H, t, 9-H, $J = 7.5$ Hz), −2.90 (s, 2H, pyrrole ring). IR (KBr pellets, ν_{max}/cm^{-1}): 3313 (porphyrin N–H), 2953–2854 (C–H), 1720 (carboxyl, C=O), 1638.2 (C=O), 1598.3 (C=C), and 1260–1220 (Ar–O–C) cm^{-1}. UV-Vis. (CH_2Cl_2, λ_{max} (nm), ε ($(mol\,L^{-1})^{-1}\,cm^{-1}$)): 419 ($1.16 \times 10^5$), 550 ($5.97 \times 10^3$), 597 ($2.13 \times 10^3$), and 646 ($1.21 \times 10^3$). ES-MS: m/z 1045.20 (M^+).

2.5.3. 5-(4-Fluoresceinhexyloxy)phenyl-10,15,20-tri(4-chloro)phenylporphyrin (Fl-HPTCPP). Fl-HPTCPP was prepared in a similar way to that of Fl-HPTTP except for 5-(4-bromohexyloxy)phenyl-10,15,20-tri(4-chloro)phenylporphyrin (BrHPTCPP) instead of BrHPTTP. The yield of Fl-HPTCPP was 53.6%. Elemental Anal. Calcd for $C_{70}H_{49}N_4O_6Cl_3$ (%): C, 73.2; H, 4.3; N, 4.9. Found (%): C, 72.5; H, 4.1; N, 4.8. ^{1}H NMR (500 Hz, DMSO, ppm): δ 11.18 (1H, s, COOH), 8.80–8.96 (8H, m, 6-H), 8.1–8.6 (6H, d, 4-H, $J = 8.2$ Hz), 7.86–7.98 (2H, d, 2-H, $J = 7.6$ Hz), 7.80–7.84 (8H, m, 1,3,5-H), 7.20–7.50 (4H, d, 10,11,12-H, $J = 8.2$ Hz), 6.16–6.90 (6H, m, 13-H), 3.95–4.50 (2H, t, 7-H, $J = 6.6$ Hz), 3.40 (8H, t, 8-H, $J = 8.0$ Hz), 1.96 (2H, t, 9-H, $J = 7.3$ Hz), −2.90 (s, 2H, pyrrole ring). IR (KBr pellets, ν_{max}/cm^{-1}): 3310 (porphyrin N–H), 2950–2857 (C–H), 1722 (carboxyl, C=O), 1640.3 (C=O), 1600.2 (C=C), and 1263–1225 (Ar–O–C) cm^{-1}. UV-Vis. (CH_2Cl_2, λ_{max} (nm), ε ($(mol\,L^{-1})^{-1}\,cm^{-1}$)): 420 ($1.18 \times 10^5$), 550 ($5.96 \times 10^3$), 598 ($2.36 \times 10^3$), and 645 ($1.28 \times 10^3$). ES-MS: m/z 1147.50 (M^+).

2.5.4. Synthesis of Zn(Fl-HPTTP) (1), Zn(Fl-HPTPP) (2), and Zn(Fl-HPTCPP) (3). The zinc(II) complex **1**, Zn(Fl-HPTTP), was synthesized with a method similar to that described earlier [25, 29, 30]. A mixture of Fl-HPTPP (105 mg), Zn $(OAc)_2$ (1.1 g), $CHCl_3$ (30 cm^3), and HAc (20 cm^3) was first stirred for 5 min at room temperature. Then the reaction mixture was maintained under reflux for 3 h at 60°C. After this, the mixture was diluted with another 20 cm^3 $CHCl_3$ and washed with water (6 × 50 cm^3).

Then it was dried with anhydrous Na_2SO_4 and concentrated *via* rotary evaporation. The residue was then chromatographed on a silica gel column using $CHCl_3 : CH_3OH = 18 : 1$(V/V) mixture as eluent and yielded a purple solid. The yield of **1** was 93.5%. Elemental Anal. Calcd for $C_{73}H_{56}N_4O_6Zn$ (%): C, 76.2; H, 4.87; N, 4.87. Found (%): C, 76.10; H, 4.82; N, 4.85. ^{1}H NMR (500 Hz, DMSO, ppm): δ 11.12 (1H, s, COOH), 8.73–8.90 (8H, m, 6-H), 8.0–8.4 (6H, d, 4-H, $J = 8.0$ Hz), 7.85–7.96 (2H, d, 2-H, $J = 7.6$ Hz), 7.80–7.83 (17H, m, 1,3,5-H), 7.20–7.53 (4H, d, 10,11,12-H, $J = 6.8$ Hz), 6.20–6.70 (6H, m, 13-H), 3.88–4.45 (2H, t, 7-H, $J = 7.9$ Hz), 3.40 (8H, t, 8-H, $J = 8.0$ Hz), 1.90 (2H, t, 9-H, $J = 7.5$ Hz). IR (KBr pellets, ν_{max}/cm^{-1}): 2920.4–2864 (C–H), 1725.3 (carboxyl, C=O), 1638.2 (C=O), 1590.6 (C=C), and 1259–1212 (Ar–O–C) cm^{-1}; UV-Vis. (CH_2Cl_2, λ_{max} (nm), ε ($(mol\,L^{-1})^{-1}\,cm^{-1}$)): 420 ($1.13 \times 10^5$), 551 ($5.90 \times 10^3$), and 596 ($2.12 \times 10^3$); ES-MS *(m/z)*: M^+, 1149.40.

Compound **2** was prepared in a similar way to that of **1** except for Fl-HPTPP instead of Fl-HPTTP. Yield: 94.3%. Elemental Anal. Calcd for $C_{70}H_{50}N_4O_6Zn$ (%): C, 72.26; H, 3.64; N, 7.02. Found (%): C, 72.10; H, 3.55; N, 6.96. ^{1}H NMR (500 Hz, DMSO, ppm): δ 11.16 (1H, s, COOH), 8.73–8.90 (8H, m, 6-H), 8.0–8.4 (6H, d, 4-H, $J = 8.1$ Hz), 7.85–7.96 (2H, d, 2-H, $J = 7.8$ Hz), 7.80–7.83 (11H, m, 1,3,5-H), 7.20–7.53 (4H, d, 10,11,12-H, $J = 7.2$ Hz), 6.20–6.70 (6H, m, 13-H), 3.88–4.45 (2H, t, 7-H, $J = 8.0$ Hz), 3.40 (8H, t, 8-H, $J = 7.2$ Hz), 1.90 (2H, t, 9-H, $J = 6.8$ Hz). IR (KBr pellets, ν_{max}/cm^{-1}): 2923.4–2860 (C–H), 1722.3 (carboxyl, C=O), 1636.6 (C=O), 1592.9 (C=C), and 1258–1216 (Ar–O–C) cm^{-1}; UV-Vis. (CH_2Cl_2, λ_{max} (nm), ε ($(mol\,L^{-1})^{-1}\,cm^{-1}$)): 420 ($1.20 \times 10^5$), 551 ($5.95 \times 10^3$), and 596 ($2.31 \times 10^3$); ES-MS (*m/z*): M^+, 1107.30.

Compound **3** was prepared in a similar way to that of **1** except for Fl-HPTCPP instead of Fl-HPTTP. Yield: 93.2%. Elemental Anal. Calcd for $C_{70}H_{47}N_4O_6Cl_3Zn$ (%): C, 69.4; H, 3.9; N, 4.6. Found (%): C, 69.0; H, 3.6; N, 4.3. ^{1}H NMR (500 Hz, DMSO, ppm): δ 11.18 (1H, s, COOH), 8.80–8.90 (8H, m, 6-H), 8.0–8.5 (6H, d, 4-H, $J = 8.1$ Hz), 7.86–7.97 (2H, d, 2-H, $J = 7.7$ Hz), 7.80–7.83 (8H, m, 1,3,5-H), 7.20–7.50 (4H, d, 10,11,12-H, $J = 7.6$ Hz), 6.16–6.90 (6H, m, 13-H), 3.95–4.50 (2H, t, 7-H, $J = 7.2$ Hz), 3.40 (8H, t, 8-H, $J = 7.8$ Hz), 1.96 (2H, t, 9-H, $J = 6.6$ Hz). IR (KBr pellets, ν_{max}/cm^{-1}): 2950–2870 (C–H), 1729 (carboxyl, C=O), 1641.3 (C=O), 1601.3 (C=C), and 1260–1225 (Ar–O–C) cm^{-1}. UV-Vis. (CH_2Cl_2, λ_{max} (nm), ε ($(mol\,L^{-1})^{-1}\,cm^{-1}$)): 420 ($1.18 \times 10^5$), 549 ($5.91 \times 10^3$), 598 ($2.36 \times 10^3$). ES-MS: *m/z* 1210.60 (M^+).

3. Results and discussion

3.1. *Synthesis and characterization*

Fluorescein-porphyrin hybrids (Fl-HPTTP, Fl-HPTPP, and Fl-HPTCPP) were synthesized according to a similar procedure with previously published method [28–31]. They show good solubility in common organic solvents, e.g., dichloromethane, chloroform, DMSO, and DMF. The pure compounds were characterized by IR, ^{1}H NMR, ESI-MS, and UV-Vis spectra along with elemental analysis.

The IR spectra of fluorescein-porphyrin hybrids clearly indicated the presence of porphyrin and fluorescein with characteristic frequencies of porphyrin and fluorescein observed at 3315 (porphyrin N–H), 2950–2858 (C–H), 1720–1725 (carboxyl, C=O), 1636–1640 (C=O), 1598.3 (C=C), and 1258–1225 (Ar–O–C) cm^{-1}, respectively [29–31].

Table 1. UV-Vis spectral data of ligands and complexes.

	λ_{max} (nm)				
Compound	Soret band		*Q* band		
Fl-HPTTP	420	518	550	598	645
Fl-HPTPP	419	519	551	597	646
Fl-HPTCPP	420	518	550	598	645
Zn(Fl-HPTTP)	420	–	548	598	–
Zn(Fl-HPTPP)	420	–	550	597	–
Zn(Fl-HPTCPP)	420	–	549	598	–

Table 1 presents the UV-Vis spectra of Fl-HPTTP, Fl-HPTPP, and Fl-HPTCPP and their zinc complexes. The spectrum of ligands has a strong absorption centered at 419 nm or 420 nm and four other peaks centered at 519, 550, 597, and 646 nm. The peak at 418 or 420 nm is the Soret band arising from the $a_{1u}(\pi)$–$e_g^*(\pi)$ transition and the other four absorptions are attributed to the *Q* bands of the $a_{2u}(\pi)$–$e_g^*(\pi)$ transition [27–30]. The spectrum clearly identifies the porphyrinic chromophores of Fl-HPTTP, Fl-HPTPP, Fl-HPTCPP, and their zinc complexes.

The ^{1}H-NMR, UV-Vis, IR, ESI-MS, and elemental analysis were in agreement with the structures of Fl-HPTTP, Fl-HPTPP, and Fl-HPTCPP (scheme 1). The characteristic proton signals at 11.16–11.22 ppm attributed to –COOH were observed in the ^{1}H NMR spectra of Fl-HPTTP, Fl-HPTPP, and Fl-HPTCPP, indicating that the carboxyls on fluorescein are free and did not react with –Br on the porphyrin ring to form ester bonds. These are similar to values reported previously [28–31].

The zinc fluorescein-porphyrin complexes were synthesized by metalation with $Zn(OAc)_2$ in $CHCl_3$ in high yields.

Porphyrin N–H at 3315 cm in IR spectra of the porphyrins were absent in **1**, **2**, and **3**, indicating deprotonation of the porphyrin ring prior to coordination [28, 30, 31].

The new fluorescein-porphyrinatozinc(II) complexes showed electronic spectra typical of metalloporphyrins with *Q* bands (table 1). *Q* bands of the zinc complexes in comparison with metal-free ligands have only two absorptions at 550 and 598 nm. This is typical of porphyrins on going from the metal-free ligands to their Zn complexes, due to an increase of symmetry of the macrocycle, indicating coordination of porphyrin nitrogen to zinc [32, 33].

The ^{1}H NMR spectra of zinc complexes are in excellent agreement with the proposed structures. The chemical shifts of the porphyrin ring protons of −2.90 ppm for **1**, **2**, and **3** in comparison with their metal-free ligands affirm that ligands were coordinated to metal.

In addition, zinc complexes were characterized on the basis of elemental analyses and mass spectral data, confirming the proposed structures. The molecular ion peaks of zinc complexes at *m*/*z* 1149.40, 1107.30, and 1210.60, respectively, were obtained by ESI-MS. The determined molecular weights were consistent with expected values.

3.2. *DNA-binding properties*

3.2.1. Electronic absorption titration. Electronic absorption spectroscopy is employed to determine the binding of complexes with DNA. Complex bound to DNA through

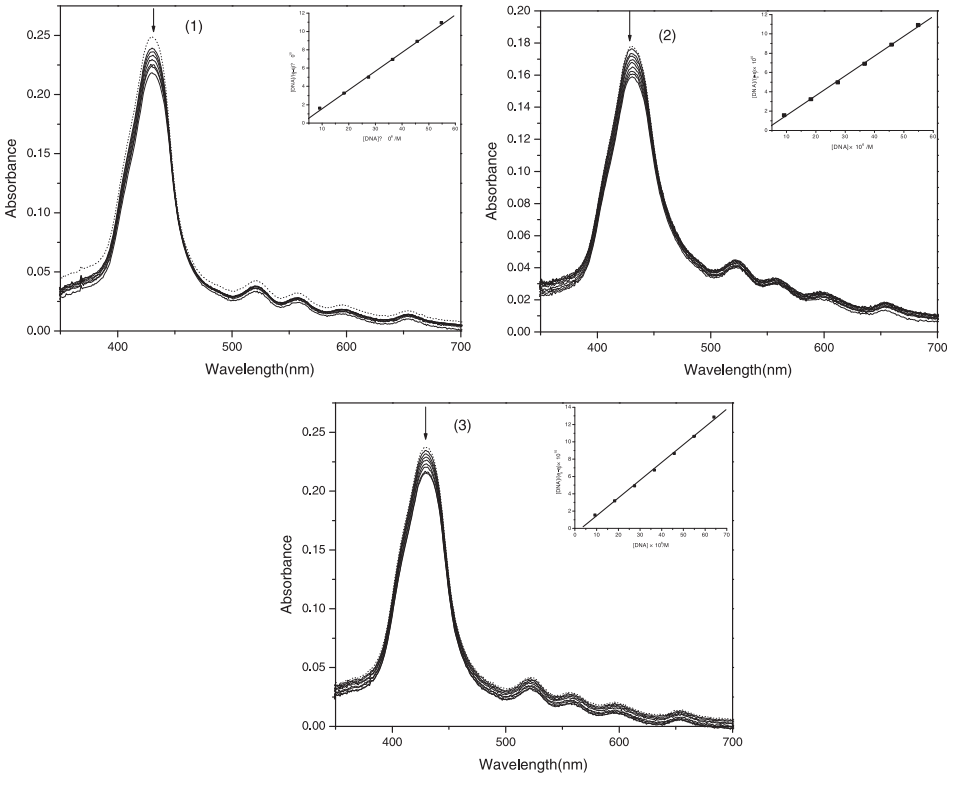

Figure 1. Absorption spectra of **1** (1), **2** (2), and **3** (3) in Tris-HCl buffer upon increasing amounts of *ct*-DNA. [Zn(Fl-Por)] = 20 μmol L^{-1}, [DNA] = (0–100) μmol L^{-1}. The arrows show the absorbance change upon increasing DNA concentration. Inset: Plots of $[DNA]/(\varepsilon_b - \varepsilon_f)$ *vs.* [DNA] for absorption titration of DNA with the complex.

intercalation usually results in hypochromism and red shift (bathochromism), due to stacking interaction between aromatic chromophore and the base pairs of DNA. The extent of the hypochromism is commonly consistent with the strength of intercalative interaction [35, 36].

In figure 1, absorption spectra of the fluorescein-porphyrinatozinc(II) complexes **1**, **2**, and **3** (at a constant concentration) are shown in the absence and presence of *ct*-DNA. Upon increasing the *ct*-DNA concentration, the hypochromism and bathochromic shift for **1** at 420 nm are 26.5% and 3 nm, respectively, at a [DNA]/[Zn(Fl-Por)] ratio of 10. However, under the same condition, with increasing *ct*-DNA concentration, **2** exhibits the hypochromism of about 20.3% at 419 nm, with a red shift 2 nm at a [DNA/[Zn(Fl-Por)] ratio of 7 and **3** exhibits the hypochromism of about 19.0% at 420 nm, with a red shift 2 at a [DNA]/[Zn(Fl-Por)] ratio of 9. According to previous reported results [37, 38], we believe that **1**, **2**, and **3** interact with DNA by intercalation.

In order to compare quantitatively the binding strength of these complexes with DNA, the intrinsic binding constants K_b were calculated by monitoring the changes of absorbance in the ligand transfer bands, with increasing amounts of *ct*-DNA. The intrinsic binding constants K_b obtained for **1**, **2**, and **3** were 4.27×10^5 $(\text{mol L}^{-1})^{-1}$, 3.25×10^5 $(\text{mol L}^{-1})^{-1}$, and 2.90×10^5 $(\text{mol L}^{-1})^{-1}$, respectively. Such values of intrinsic

binding constants are smaller than reported complexes such as zinc complex containing cationic porphyrin–anthraquinone hybrid [37], suggesting that the interactions of **1**, **2**, and **3** with DNA are medium strength intercalation. The difference may be due to the electronic effects of the substituent cationic group introduced on the porphyrin ring of porphyrin–anthraquinone hybrids, which may increase the DNA-binding affinity. To fully understand the mechanism involved in the interaction of these three complexes with DNA, further investigation will be needed.

The K_b decreases in the order **1** > **2** > **3**. The K_b value of **1** is larger than that of **2** and **3** due to the electron-pushing of $-CH_3$ on the 10-, 15-, and 20-positions of the porphyrin ring for **1**, increasing the DNA-binding affinity [37–39]. Complex **3** exhibits much weaker binding to double-helical DNA than **1** and **2** due to the introduction of three chlorines on the 10-, 15-, and 20-positions of the porphyrin ring. Owing to their electron-withdrawing effects, the electron density of the aromatic chromophore of fluorescein-porphyrin which may intercalate into base pairs of *ct*-DNA in **3** will be altered, resulting in the lower K_b. The DNA-binding affinities of these fluorescein-porphyrinatozinc(II) complexes are associated with the electronic effects of the substituents introduced on the porphyrin ring of the ligands.

3.2.2. Viscosity measurements. To further clarify the binding interaction between complexes and DNA, viscosity measurements were carried out on *ct*-DNA by varying the concentration of the added complexes. Hydrodynamic measurements which are sensitive to length increase (e.g., viscosity, sedimentation) are regarded as the least ambiguous and the most critical tests of binding in solution in the absence of crystallographic structure data [36–40]. A classical intercalative mode causes a significant increase in viscosity of DNA solution due to increase in separation of base pairs at intercalation sites and hence an increase in overall DNA length. In contrast, partial, non-classical intercalation of compounds could bend (or kink) the DNA helix and reduce its effective length and, concomitantly, its viscosity [36, 41–43].

The effects of **1**, **2**, **3**, and EB on the viscosity of *ct*-DNA are shown in figure 2. As seen in figure 2, upon increasing the amounts of **1**, **2**, and **3**, the relative viscosity of DNA increases steadily. The increasing viscosity is **1** > **2** > **3**. The viscosity results thus provide strong evidence for the interaction of **1**, **2**, and **3** with DNA by intercalation.

3.2.3. Fluorescence spectroscopic studies. Emission spectra of all three complexes in the absence and presence of *ct*-DNA are shown in figure 3. Upon addition of *ct*-DNA, the emission intensity increases steadily and reaches 3.7 times larger than that in the absence of DNA for **1**, 3.12 times for **2**, and 2.4 times for **3** at the ratio of [DNA]/[Zn(Fl-Por)] = 150. This implies that the complexes intercalate into the base pairs of DNA and are protected by DNA efficiently, since the hydrophobic environment provided by DNA can protect them from water and thus prolong the luminescence lifetime and lead to an increase in the emission intensity [33–36].

According to the Stern–Volmer equation [34, 35]:

$$I/I_0 = 1 + kr,$$

where I_0 and I are the fluorescence intensities in the absence and presence of fluorescein-porphyrinatozinc(II) complexes, respectively. K is a linear Stern–Volmer quenching

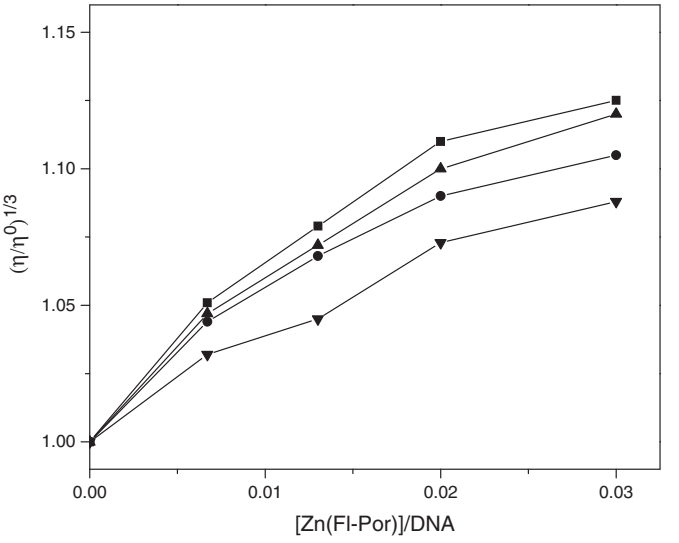

Figure 2. Effect of increasing amounts of EB (■), **1** (▲), **2** (●), and **3** (▼) on the relative viscosities of *ct*-DNA at 25 ± 0.1°C. The total concentration of DNA is 0.5 mmol L^{-1}.

constant and *r* is the ratio of total concentration of DNA to that of fluorescein-porphyrinatozinc(II) complexes. The quenching plots (inset in figure 3) illustrate that quenching of fluorescein-porphyrinatozinc(II) complexes by DNA are in good agreement with the linear Stern–Volmer equation, which also proves that fluorescein-porphyrinatozinc(II) complexes bind to DNA. With the plot of I/I_0 *versus* [Zn(Fl-Por)]/[DNA], *K* is given by the ratio of the slope to intercept. The *K* values for **1**, **2**, and **3** are 15.6, 13.2, and 9.3, respectively. The data indicate that the interaction of **1** with DNA is the strongest, followed by **2**, and then **3**, consistent with that observed by electronic absorption.

3.2.4. Thermal denaturation studies. Thermal behaviors of DNA in the presence of compounds can give insight into their conformational changes when temperature is raised and offer information about the interaction strength of complexes with DNA. Normally, when the temperature in solution increases, the double-stranded DNA will gradually dissociate to single strands and generate a hyperchromic effect on the absorption spectra of DNA bases ($\lambda_{max} = 260$ nm). The melting temperature T_m, which is defined as the temperature where half of the total base pairs are unbonded, will increase considerably when intercalative binding occurs, since intercalation of the complexes into DNA base pairs causes stabilization of base stacking and hence raises the melting temperature of the double-stranded DNA [36, 40, 41].

The melting curves of *ct*-DNA in the absence and presence of **1**, **2**, and **3** are illustrated in figure 4. The T_m of *ct*-DNA in the absence of the complexes is 62.2 ± 0.2°C. As can be seen from figure 4, when mixed with the compounds at a concentration ratio [Zn(Fl-Por)]/[DNA] of 1 : 11, the observed melting temperatures in the presence of **1**, **2**, and **3** reach 72.1 ± 0.2°C, 68.3 ± 0.2°C, and 65.7 ± 0.2°C, respectively. The largest increase in T_m ($\Delta T_m = 9.9$°C) in the presence of **1**, moderate

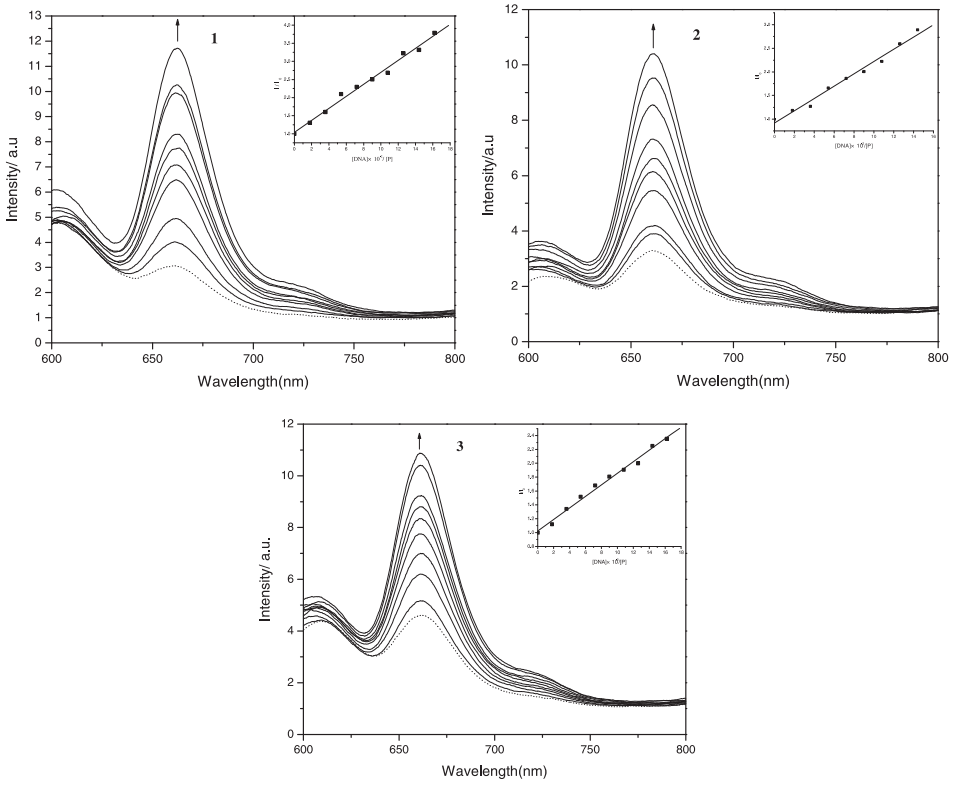

Figure 3. Emission spectra of **1** (1), **2** (2), and **3** (3) in aqueous buffer (Tris 5 mmol L^{-1}, NaCl 50 mmol L^{-1}, pH = 7.2) at 298 K in the presence (—) and absence (– – –) of *ct*-DNA. The arrows show the intensity changes upon increasing DNA concentration. Inset: Fluorescence quenching curves of fluorescein-porphyrinatozinc(II) complexes **1**, **2**, and **3** by DNA. [Zn(Fl-Por)] = 5×10^{-8} mol L^{-1}.

increase in T_m ($\Delta T_m = 6.1°C$) in the presence of **2** and smallest increase in T_m ($\Delta T_m = 3.4°C$) in the presence of **3** are comparable to those observed for classical intercalators and lend strong support for their binding with DNA by intercalation [40–43].

3.2.5. CD studies. CD spectra play an important role in the study of the interaction between porphyrin complexes and DNA as CD spectra are very sensitive to the binding modes of small molecules to DNA. The sign of the induced CD spectrum of DNA in the Soret region can be used as a sensitive signature for the binding modes of porphyrins to DNA: a positively induced CD band is indicative of external (minor groove) binding, a negatively induced CD band is produced upon intercalation and a conservative induced CD band is characteristic of outside binding [6, 41, 44, 45].

As shown in figure 5, the fluorescein-porphyrinatozinc(II) complexes do not yield CD spectra in the absence of DNA, but CD spectra were induced for the fluorescein-porphyrinatozinc(II) complexes in the presence of DNA, due to the interaction between the transition moments of the achiral porphyrin and chirally arranged DNA base transitions. Complexes **1**, **2**, and **3** show strong negative peaks centered at *ca* 440 nm

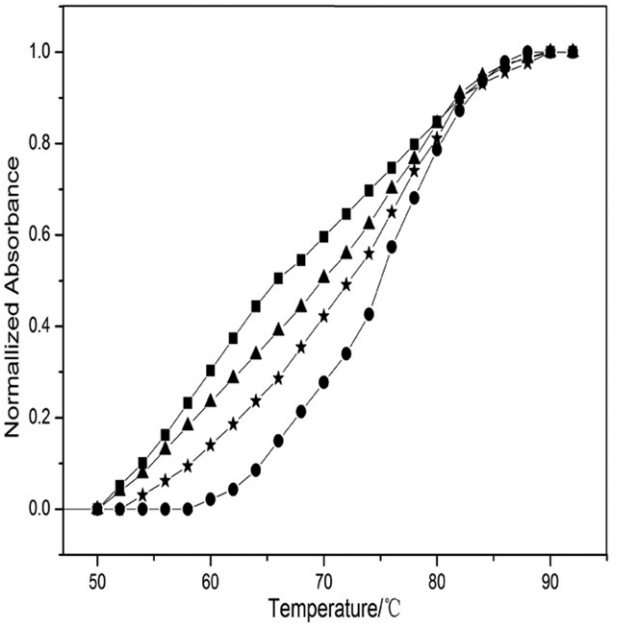

Figure 4. Melting temperature curves of *ct*-DNA in the absence (■) and presence of **1** (●), **2** (★), and **3** (▲). [Zn(Fl-Por)] = 10 μmol L^{-1}, [DNA] = 110 μmol L^{-1}.

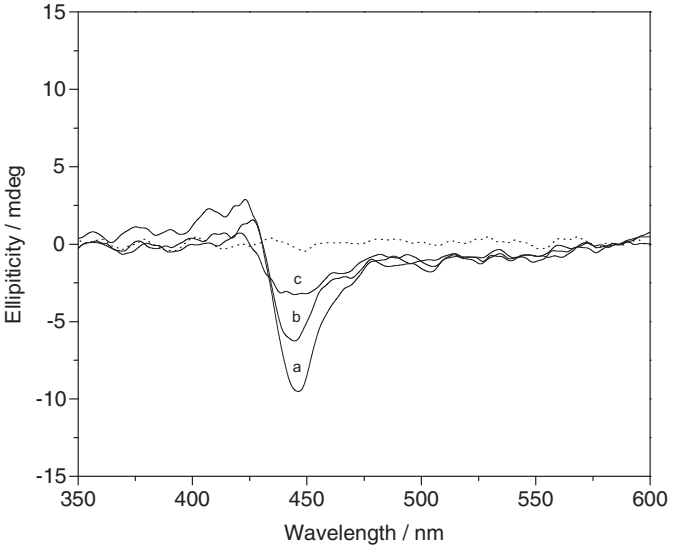

Figure 5. Induced CD spectra of **1**, **2**, and **3** in the absence (...) and presence (—) of *ct*-DNA. (a) **1** + DNA; (b) **2** + DNA; (c) **3** + DNA, [Zn(Fl-Por)] = 10 μmol L^{-1} and [DNA] = 130 μmol L^{-1}. The spectra were recorded at 25°C after samples had been incubated with *ct*-DNA for 24 h at 37°C.

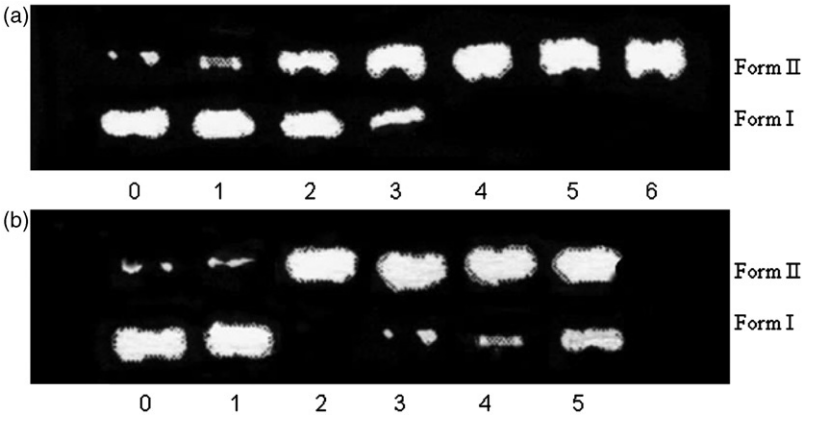

Figure 6. (a) Photoactivated cleavage of pBR 322 DNA in the presence of **1** after 60 min irradiation at 365 nm. Lane 0, DNA alone; Lanes (1–6), at 10, 20, 30, 40, 50, and 60 μmol L^{-1} **1**, respectively. (b) Photoactivated cleavage of pBR 322 DNA of **1**, **2**, or **3**. Lane 0, DNA alone; Lane 1, DNA + TPP (40 μmol L^{-1}); Lane 2, DNA + **1** (40 μmol L^{-1}); Lane 3, DNA + **2** (40 μmol L^{-1}); Lane 4, DNA + **3** (40 μmol L^{-1}); Lane 5, DNA + fluorescein (40 μmol L^{-1}).

upon binding to *ct*-DNA, suggesting that they are excellent DNA intercalators, further supporting the conclusion that **1**, **2**, and **3** interact with *ct*-DNA by intercalative modes.

3.3. *Photoinduced cleavage of pBR 322 DNA by fluorescein-porphyrinatozinc(II) complexes*

To further investigate the interactions of these complexes with DNA, photocleavage experiments were employed, in which the cleavage reaction on supercoiled plasmid DNA was monitored by agarose gel electrophoresis. When circular plasmid DNA is subject to electrophoresis, relatively fast migration will be observed for the intact supercoiled form (form I). If scission occurs on one strand (nicking), the supercoil will relax to generate a slower moving open circular form (form II). If both strands are cleaved, a linear form (form III) migrating between forms I and II will be generated [43, 46–48].

The gel electrophoretic separations of plasmid pBR 322 DNA after incubation with fluorescein-porphyrinatozinc(II) complexes and irradiation with a high pressure mercury lamp at 365 nm for 60 min are shown in figure 6. As seen in figure 6(a), no significant DNA cleavage was observed for negative controls (lane 0). With increasing concentration of **1** (lanes 1–6), the amount of form I of pBR 322 DNA diminish gradually, whereas form II increases, resulting from single strand cleavage of pBR 322 DNA.

In figure 6(b), the gel electrophoretic pattern of plasmid pBR 322 DNA is after incubation with ZnTPP (TPP = 5,10,15,20-tetraphenylporphyrin), fluorescein, or **1**, **2**, or **3**, and irradiation with white-light. No significant DNA cleavage was observed for negative controls (lane 0) and/or in the control experiment in which fluorescein-porphyrinatozinc(II) complexes was replaced by ZnTPP (lane 1). However, for **1**, **2**, and **3** (lanes 2–4), at 40 μmol L^{-1}, significant amounts of the open circular form II

were observed, indicating that these three complexes cleave pBR 322 DNA efficiently. Under comparative experimental conditions, the cleavage ability follows the order **1** > **2** > **3**, in parallel with the magnitude of their intrinsic binding constants (K_b). The cleavage experimental results thus provide another strong evidence for the substituting group on the porphyrin ring being the factor to influence their interactions with DNA. Noticeably, for fluorescein (lane 5), at 40 μmol L^{-1}, significant amounts of form II were also visible, which implies that fluorescein-porphyrinatozinc(II) complexes bind to *ct*-DNA by intercalation *via* the planar fluorescein into the base pairs of DNA. Further investigation is required to study the possible cleavage mechanisms of these three complexes.

4. Conclusions

Three fluorescein-porphyrinatozinc complexes, **1**, **2**, and **3**, were synthesized and characterized. The interaction of these three complexes with *ct*-DNA was studied using UV-Vis, fluorescence spectroscopic titration, viscosity measurements, thermal denaturation, and CD. The results suggest that **1**, **2**, and **3** interact with *ct*-DNA by intercalation. The DNA-binding affinity, K_b, values follow the order **1** > **2** > **3**. Photocleavage reactions with pBR322 supercoiled plasmid DNA exhibit significant DNA cleavage activity and the cleavage ability also follows the order **1** > **2** > **3**. The results also suggest that fluorescein-porphyrinatozinc(II) complexes bind to *ct*-DNA by intercalation *via* the planar fluorescein into the base pairs of DNA.

Acknowledgments

We gratefully acknowledge financial support for this work by Guangdong Pharmaceutical University (43540119), the National Key Research Project of China (2011zx09102-001-31), and the National Natural Science Foundation of P.R. China (No. 31070858 and 81102753).

References

[1] A.E. O'Connor, W.M. Gallagher, A.T. Byrne. *Photochem. Photobiol.*, **85**, 1053 (2009).
[2] W. Waskitoaji, T. Hyakutake, J. Kato, M. Watanabe, H. Nishide. *Chem. Lett.*, **38**, 1164 (2009).
[3] M.J. Shieh, C.L. Peng, P.J. Lou, C.H. Chiu, T.Y. Tsai, C.Y. Hsu, C.Y. Yeh, P.S. Lai. *J. Control. Release*, **7**, 200 (2008).
[4] C.T. Poon, S. Zhao, W.K. Wong, D.W.J. Kwong. *Tetrahedron Lett.*, **51**, 664 (2010).
[5] S. Mettath, B.R. Munson, R.K. Pandey. *Bioconjug. Chem.*, **10**, 94 (1999).
[6] R.F. Pasternack, E.J. Gibbs, J.J. Villafranca. *Biochemistry*, **22**, 2406 (1983).
[7] M. Yedukondalu, M. Ravikanth. *Coord. Chem. Rev.*, **255**, 547 (2011).
[8] R.J. Fiel, J.C. Howard, E.H. Mark, N.D. Gupta. *Nucleic Acids Res.*, **6**, 3093 (1979).
[9] Y. Ishikawa, N. Yamakawa, T. Uno. *Bioorg. Med. Chem.*, **10**, 1953 (2002).
[10] R.F. Pasternack, E.J. Gibbs, J.J. Villafranca. *Biochemistry*, **22**, 2406 (1983).
[11] A. D'Urso, A. Mammana, M. Balaz, A.E. Holmes, N. Berova, R. Lauceri, R. Purrello. *J. Am. Chem. Soc.*, **131**, 2046 (2009).

[12] C. Sambaiah, B. Msunier, N. Paillous. *J. Photochem. Photobiol B: Biol*., **16**, 47 (1992).
[13] G. Mehta, T. Sambaiah, B.G. Maiya, M. Sirish, A. Dattagupta. *Tetrahedron Lett*., **135**, 4201 (1994).
[14] D.T. Breslin, J.E. Coury, J.R. Anderson, L. Mcfail-Isom, Y. Kan. *J. Am. Chem. Soc*., **119**, 5043 (1997).
[15] Z.P. Li, Y.H. Xing, Y.H. Zhang, G.H. Zhou, C.G. Wang, J. Li, X.Q. Zeng, M.F. Ge, S.Y. Niu. *J. Coord. Chem*., **62**, 564 (2009).
[16] E.K. Efthimiadou, N. Katsaros, A. Karaliota, G. Psomas. *Bioorg. Med. Chem. Lett*., **17**, 1238 (2007).
[17] J. Benítez, L. Guggeri, I. Tomaz, J.C. Pessoa, V. Moreno, J. Lorenzo. *J. Inorg. Biochem*., **103**, 1386 (2009).
[18] A.A. Nejo, G.A. Kolawole, A.R. Opoku, J. Wolowska, P. O'Brien. *Inorg. Chim. Acta*, **362**, 3993 (2009).
[19] A. McCrate, M. Carlone, M. Nielsen, S. Swavey. *Inorg. Chem. Commun*., **13**, 537 (2010).
[20] A. Wolfe, G.H. Shimer, T. Meehan. *Biochemistry*, **26**, 6392 (1987).
[21] V. Vaz Serra, A. Zamarrón, M.A.F. Faustino, M.C. Iglesias-de la Cruz, A. Blázquez, J.M.M. Rodrigues, M.G.P.M.S. Neves, J.A.S. Cavaleiro, A. Juarranz, F. Sanz-Rodríguez. *Bioorg. Med. Chem*., **18**, 6170 (2010).
[22] T.M. Kelly, A.B. Tossi, D.J. McConnell, T.C. Strekas. *Nucleic Acids Res*., **13**, 6017 (1985).
[23] E.D. Sternberg, D. Dolphin, C. Bruckner. *Tetrahedron*, **54**, 4151 (1998).
[24] T.J. Dougherty, C.J. Gomer, B.W. Henderson, G. Jori, D. Kessel, M. Korbelik, J. Moan, Q. Peng. *J. Natl Cancer Inst*., **90**, 889 (1998).
[25] K. Oda, S. Ogura, I. Okura. *J. Photochem. Photobiol. B*, **59**, 20 (2000).
[26] G. Mező , L. Herényi, J. Habdas, Z. Majer, B.M. Kurdziel, K. Tóthf, G. Csík. *Biophys. Chem*., **155**, 36 (2011).
[27] R.J. Fiel. *J. Biomol. Struct. Dyn*., **6**, 1259 (1989).
[28] X.B. Yan, M. Weng, M.H. Zhang, T. Shen. *Dyes Pigm*., **36**, 259 (1998).
[29] J.Z. Lu, Y.F. Du, B. Wu, J.W. Huang, J. Jiang. *Trans. Met. Chem*., **35**, 451 (2010).
[30] J.Z. Lu, J.W. Huang, L.F. Fan, J. Liu, X.L. Chen, L.N. Ji. *Inorg. Chem. Commun*., **7**, 1030 (2004).
[31] J.Z. Lu, X.C. Tan, J.W. Huang, C.H. Dong. *Trans. Met. Chem*., **30**, 643 (2005).
[32] P. Zhao, L.C. Xu, J.W. Huang, B. Fu, H.C. Yu, L.N. Ji. *Biophys. Chem*., **135**, 102 (2008).
[33] P. Zhao, L.C. Xu, J.W. Huang, B. Fu, H.C. Yu, L.N. Ji. *Spectrochim. Acta, Part A*, **71**, 1216 (2008).
[34] P. Zhao, L.C. Xu, J.W. Huang, B. Fu, H.C. Yu, L.N. Ji. *Bioorg. Chem*., **36**, 278 (2008).
[35] J.Z. Lu, Y.F. Du, H.W. Guo. *J. Coord. Chem*., **64**, 1229 (2011).
[36] Y.F. Du, J.Z. Lu, H.W. Guo, J. Jiang. *Trans. Met. Chem*., **35**, 859 (2010).
[37] P. Zhao, J.W. Huang, L.N. Ji. *J. Coord. Chem*., **64**, 1977 (2011).
[38] P. Zhao, J.W. Huang, L.N. Ji. *Dyes Pigm*., **83**, 81 (2009).
[39] S. Satyanarayana, J.C. Dabrowiak, J.B. Chaires. *Biochemistry*, **32**, 2573 (1993).
[40] R. Kuroda, H. Tanaka. *J. Chem. Soc., Chem. Commun*., 1575 (1994).
[41] H.T. Daryono, M. Shunsuke, A. Takehiro, Y. Naoki, I. Hidenari. *J. Inorg. Biochem*., **85**, 219 (2001).
[42] R.F. Pasternack, E.J. Gibbs, J.J. Villafrancas. *Biochemistry*, **22**, 2406 (1983).
[43] E. Nyarko, M. Tabata. *J. Porphyrins Phthalocyanines*, **5**, 873 (2001).
[44] B. Chen, W. Qin, P. Wang, T. Tian, H.J. Ma, X.P. Cao, X.J. Wu, X. Zhou, X.L. Zhang, F. Liu, F. Zheng, X. Li. *Bioorg. Med. Chem. Lett*., **13**, 3731 (2003).
[45] T.F. Al-Azemi, M. Vinodh. *Tetrahedron*, **67**, 2585 (2011).
[46] B.E. Smith, T.D. Lash. *Tetrahedron*, **66**, 4413 (2010).
[47] A. McCrate, M. Carlone, M. Nielsen, S. Swavey. *Inorg. Chem. Commun*., **13**, 537 (2010).
[48] J.K. Barton, A.L. Raphael. *J. Am. Chem. Soc*., **106**, 2466 (1984).